Measured RF Backscatter Power Statistics in Indoor Sensing

Dmitry Chizhik[(1)], Jakub Sapis[(1)], Jinfeng Du[(1)], Reinaldo A. Valenzuela[(1)], Abhishek Adhikari[(2)], John Drogo[(2)],Gil Zussman[(2)], Manuel A. Almendra[(3)], Mauricio Rodriguez[(3)], and Rodolfo Feick[(4)]

(1) Nokia Bell Labs, Murray Hill, NJ 07974, USA (dmitry.chizhik@nokia-bell-labs.com)
(2) Columbia University, New York, NY, USA
(3) Pontificia Universidad Católica de Valparaíso, Valparaíso, Chile
(4) Universidad Técnica Federico Santa María, Valparaíso, Chile

***Abstract*— Backscatter power measurements are collected to characterize indoor radar clutter in monostatic sensing applications. A narrowband 28 GHz sounder used a quasi-monostatic radar arrangement with an omnidirectional transmit antenna illuminating an indoor scene and a spinning horn receive antenna offset vertically (less than 1 m away) collecting backscattered power as a function of azimuth. Power variation in azimuth around the local average is found to be within 1 dB of a lognormal distribution with a standard deviation of 6.8 dB. Backscatter azimuth spectra are found to be highly variable with location, with cross-correlation coefficients on the order of 0.3 at separations as small as 0.1 m. These statistics are needed for system-level evaluation of RF sensing performance.**

Index terms— **sensing, backscatter.**

I. INTRODUCTION

There is an increasing interest [1][2][3][4] in the use of communication signals for sensing, often termed Joint/Integrated Communications and Sensing (JCAS or ISAC). Often the goal is to detect and localize a static or moving object, termed "target", such as a person, vehicle, robot, or UAV, in the presence of the rest of the environment, the response to which is termed "clutter". Indoor applications include [5] detection of people, robots in indoor spaces for safety (collision avoidance in factories, frail person in room monitoring in healthcare settings), security (intruder detection). In these applications, the person/robot is either standing or lying on the floor.

Clutter echoes are often stationary, e.g., buildings outdoors, walls and furniture indoors but may also include moving objects such as people, vehicles, as well as vegetation and various street furniture that sway with the wind. Sensing scenarios of interest include monostatic, with collocated transmitter/receiver measuring backscatter, e.g., a single base station or terminal, as well as bi-static where transmitter and receiver are separated, e.g., signal traveling from one base station to another, scattering along the way. Various use cases for joint communication and sensing are under consideration by the 3GPP [5].

Algorithms for detection, localization and, possibly, classification, of objects need to be tested in realistic scenarios, requiring representative models of both clutter and target.

It is desirable for the model to be easily implementable. Standardized models such as 3GPP TR 38.901 [6] describe communication models which have been adopted in proposals for statistical channel models for communications and sensing [8][9][10]. While such formulations are very general, determination of properties such as strength of backscatter remains open, particularly for clutter. Clutter may be viewed as either an extended object or a collection of many objects. Backscatter from clutter is then critically dependent on the number and scattering strength of such objects, as well as multiple scattering from them. This information is not available from current 3GPP communication channel models or single object target models developed in radar.

Deterministic models, such as ray tracing, are general enough to be used in both monostatic and bi-static arrangements [16]. Hybrid models such as quasi-deterministic models [14][15] (see also references therein) supplement site-specific cluster/ray generation from ray tracing with stochastic components to capture the complexity and uncertainty of the environment and the targets. Aside from issues with accuracy [7][11], such models require use of specialized, often licensed, software making standardization difficult.

Models developed for communication channels are often inapplicable to many of the sensing tasks. For example, monostatic RF sensing measures backscatter, not of interest in communication channels where the signal of interest goes from transmitter to a well separated receiver.

In this work we propose a measurement-based monostatic indoor backscatter model. Narrowband measurements of backscatter power as a function of azimuth at 28 GHz were collected in 3 cities in 251 indoor locations from 27 rooms of different sizes, allowing formulation of a model for indoor backscatter validated though a statistically significant data set, in environments containing both metal and dielectric materials. This data was used [17] to report that average measured clutter

Dmitry Chizhik, Jinfeng Du, Jakub Sapis and Reinaldo A. Valenzuela are with Nokia Bell Labs, Murray Hill, NJ 07974, USA (e-mail: dmitry.chizhik@nokia-bell-labs.com, jinfeng.du@nokia-bell-labs.com, jakub.sapis@nokia-bell-labs.com, reinaldo.valenzuela@nokia-bell-labs.com), Abhishek Adhikari, Gil Zussman, are with Columbia University, New York, NY, abhishek.adhikari@columbia.edu, gil.zussman@columbia.edu, Manuel A. Almendra and Mauricio Rodgriguez is with Pontificia Universidad Católica de Valparaíso, Valparaíso, Chile, (email: manuel.almendra.v@mail.pucv.cl, mauricio.rodriguez.g@pucv.cl), Rodolfo Feick is with Universidad Técnica Federico Santa María, Valparaíso, Chile (email: rodolfo.feick@usm.cl)

backscatter power ratio generally decreases with increasing room size, well modeled by a simple function of distance, similar to free space path loss.

In present work, the backscatter power ratio is represented as varying over azimuth about an average, with variation statistics derived from measurements. Azimuthal power spectra measured at locations every 10 cm allowed an assessment of variability at closely spaced locations. Key results include:

- Variation of clutter backscatter about its local average is within 1 dB of a lognormal distribution
- Backscatter azimuth spectra are found to be highly variable with location, with cross-correlation coefficients on the order of 0.3 at separations as small as 0.1 m.

II. BACKSCATTER FROM A CLUTTER

For the quasi-monostatic antenna arrangement studied here, the transmit and receive antennas are (nearly) collocated and received radar power of a signal backscattered from an object R meters away with effective backscatter cross-section (RCS) σ_{back} is given by the radar equation [12]:

$$P_{\text{back}} = \frac{\lambda^2 \sigma_{\text{back}} P_{\text{T}} G_{\text{T}} G_{\text{R}}}{(4\pi)^3 R^4} \tag{1}$$

where λ is carrier wavelength, P_{T} is the transmit power, G_{T} and G_{R} are the antenna gains.

In the case of an extended scatterer, such as a rough wall or a dense collection of distributed scatterers, (1) generalizes [12] to an integral over the surface of the extended scatterer:

$$P_{\text{clut}} = \frac{\lambda^2 P_{\text{T}}}{(4\pi)^3} \iint dA \; G_{\text{T}}(\Omega) G_{\text{R}}(\Omega) \frac{\gamma_{\text{back}}(\Omega)}{R^4} \tag{2}$$

Where $\gamma_{\text{back}}(\Omega)$ is a (unit-less) backscattering cross-section of the clutter surface per unit area, as a function of illumination angle Ω.

Backscatter power ratio for clutter:

$$P_{\text{back}} = \frac{P_{\text{clut}}}{P_{\text{T}}} \tag{3}$$

is characterized via measurement in the following section.

III. MEASUREMENT DESCRIPTION

The sensing measurement set-up was adopted from a narrowband channel sounder [13]. The resulting sensing sounder consisted of a transmitter and receiver placed on the same cart, separated vertically, isolated from each other by absorbing foam to avoid contamination of receive signals with direct path arrival. The measurement system is meant to emulate an indoor access point (AP) transmitter with a nearly collocated sensing receiver, both placed within 2 m above the floor, with antennas illuminating the interior space where people/robots might be, also within 2 m above the floor. A 28 GHz CW tone at 22 dBm was transmitted from an omnidirectional antenna, with vertical beamwidth of about 70°. This transmitter was placed on a lower shelf of a plastic cart (Fig. 1), 0.4 m above the floor to illuminate the surrounding area uniformly in all azimuthal directions. A spinning directional receive antenna, placed on an upper shelf of the cart, 1.1 m above the floor, was a 24 dBi horn with 10° half-power beamwidth performing a full azimuthal rotation every 200 ms. Received power is sampled at 740 samples/sec and recorded, together with azimuth of the antenna aim. Calibration measurements were carried out to assure minimal scatter from the cart, with multiple layers of absorbing foam to attenuate the direct Tx-Rx signal path.

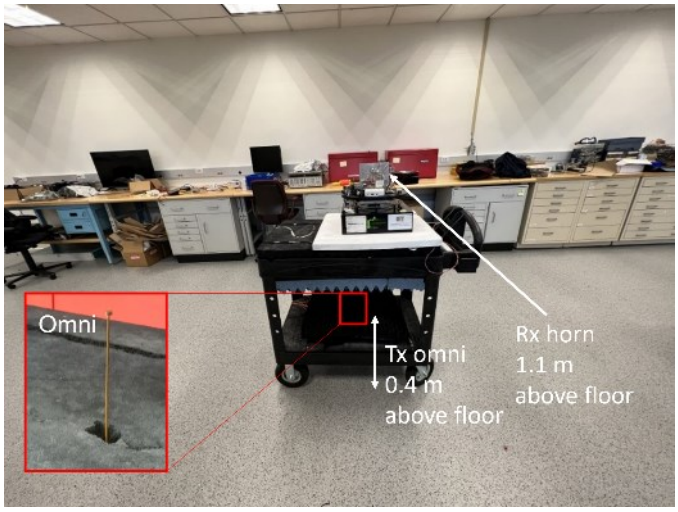

Fig. 1. 28 GHz narrowband backscatter radar arrangement, with omnidirectional Tx antenna on lower cart shelf illuminating the scene and a spinning horn receiver collecting backscatter power vs. azimuth on top cart shelf.

The data was collected in 3 different building types in New York City, New Jersey office building and a university building in Chile. The cart was placed in 251 locations from 27 rooms of varying sizes, from 3x3 m offices to 20x30 m cafeteria, collecting backscatter azimuth spectra like one shown in Fig. 2. Room materials varied, with some rooms containing metal furniture along the walls, others with primarily wood furniture and drywall walls. Some rooms had metal furniture and metalized windows, others wooden furniture and plain glass windows. Measured clutter backscatter power ratio as a function of azimuth is analyzed to create a statistical backscatter model. The backscatter power ratio is represented statistically as an average over azimuth and variation around that azimuth. At each location, an azimuthal average of backscatter power ratio is computed from measurements as:

$$\langle P_{\text{back}}(\phi) \rangle_{\phi} = \frac{\langle P_{\text{clut}}(\phi) \rangle_{\phi}}{P_{\text{T}} G_{T}} \tag{4}$$

indicated as a dashed circle in Fig. 2. G_{T} is the gain of the transmit antenna, G_{T}=1 for the antenna used here. Thus (4) is the average of (3). Backscattered clutter power ratio (4) was shown in [17] to be independent of the antenna pattern of the (high gain) receive antenna. This makes (4) independent of

measurement apparatus here and characteristic of the environment under study. The observed average backscatter value varied from location to location. The average backscatter power is found to decrease as the room size increases. It is also observed that clutter backscatter in rooms with metal clutter is generally higher than from dielectric clutter. In [17] a simple deterministic formula for average clutter power, dependent on average distance to clutter, was derived. In current work, we report on the observed deviations of backscattered power from that average as antenna rotates.

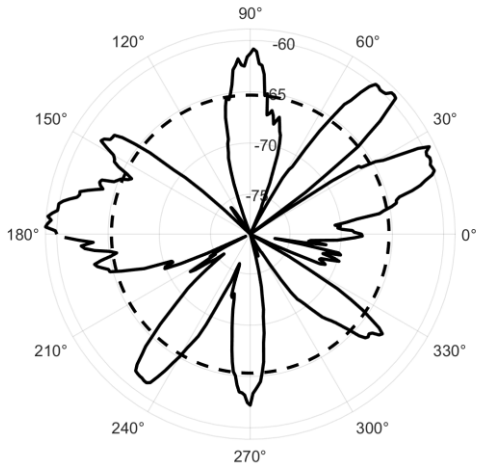

Fig. 2. Sample measured backscattered power ratio vs. azimuth. Dashed line is average backscattered power ratio (4)

IV. OBSERVED AZIMUTH VARIATION STATISTICS

As illustrated in Fig. 2, measured backscattered power exhibits variation with azimuth around its local average. The distribution of observed power variations relative to observed average power $\left\langle P_{\text{clut}}(\phi)\right\rangle_{\phi}$ is plotted as a solid line in Fig. 3. The power $\mathrm{P}_{\text{rel}}(\phi)$ relative to local average

$$\mathrm{P}_{\text{rel}}(\phi)=\frac{P_{\text{clut}}(\phi)}{\left\langle P_{\text{clut}}(\phi)\right\rangle_{\phi}} \tag{5}$$

is seen in Fig. 3 to be within 1 dB of the lognormal distribution

$$\begin{aligned} &10\log_{10}\left(\mathrm{P}_{\text{rel}}(\phi)\right)\sim N(\mu,\sigma),\ \sigma=6.8\text{ dB},\\ &\mu=-10\log_{10}e^{(0.1*\ln(10)*\sigma)^2/2}=5.3\text{ dB} \end{aligned} \tag{6}$$

The standard deviation σ is the adjustable parameter, while the mean μ is a function of σ, to assure $\left\langle \mathrm{P}_{\text{rel}}(\phi)\right\rangle_{\phi}=1$, which follows from normalization (5).

Spatial varibility of observed azimuth spectra was examined in a lab, with locations along a 1 m long line segment every 10 cm, for a total of 11 azimuthal spectra. Cross-correlation coefficient $\rho(d_2-d_1)$ of azimuthal spectra was computed for different separations d_2-d_1 using measured spectra $P(\phi,d_n)$ at locations d_n as:

$$\begin{aligned} &\rho(d_2-d_1)=\left\langle p(\phi,d_2)\,p(\phi,d_1)\right\rangle,\\ &p(\phi,d_n)\equiv\frac{P(\phi,d_n)-\left\langle P(\phi,d_n)\right\rangle}{\left\langle\left(P(\phi,d_n)-\left\langle P(\phi,d_n)\right\rangle\right)^2\right\rangle^{1/2}},\ n=1,2 \end{aligned} \tag{7}$$

Cross-correlation coefficient computed from data is plotted in Fig 4 as a function of location separation $\left|d_2-d_1\right|$. The correlation coefficient is seen to drop to about 0.3 for location separation as small as 0.1 m, indicating rapid variation in azimuthal spectra even with small displacement.

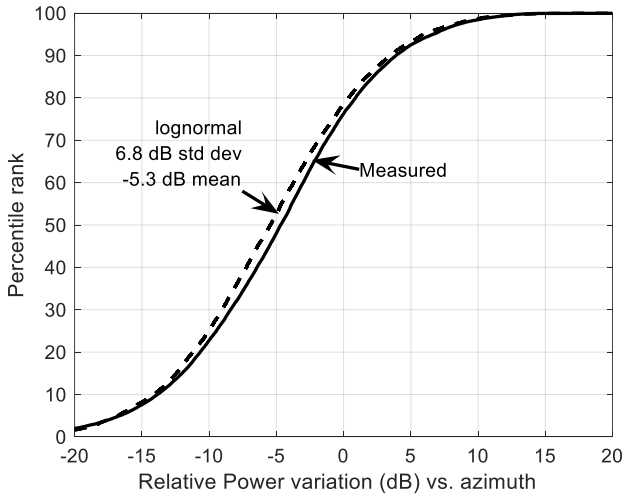

Fig. 3. Cumulative distribution of azimuthal variation of measured backscattered power ratio around local average.

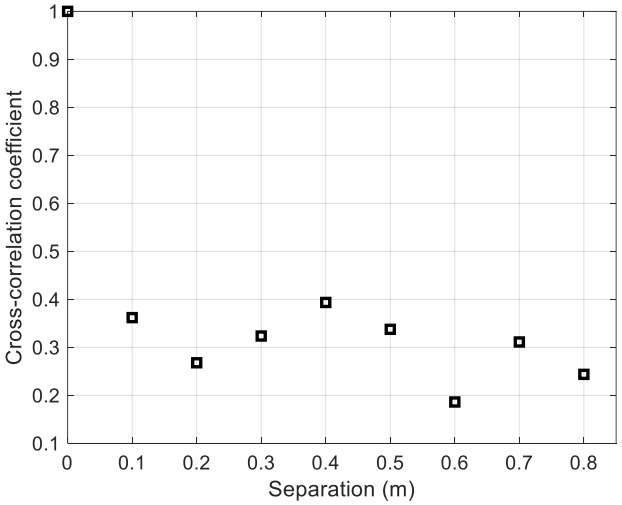

Fig. 4. Correlation of measured azimuthal spectra (7) as a function of separation.

V. CONCLUSIONS

A simple statistical monostatic radar channel model for indoor clutter is developed for indoor applications, requiring only a handful of parameters, including room dimensions, materials and measurement-derived standard deviation of azimuthal power variation. A narrowband 28 GHz sounder was used in a quasi-monostatic antenna arrangement with an omnidirectional transmit antenna illuminating the scene and a spinning horn receive antenna collecting backscattered power as a function of azimuth. Distribution of power variation in azimuth around this average is reproduced within 1 dB by a random azimuth spectrum with a lognormal amplitude distribution and random phase. Such statistical models are essential for large-scale system-level evaluation of RF sensing performance.

VI. ACKNOWLEDGEMENTS

Thanks to David Chen (Stuyvesant High School) and Timothy Wang (University of Michigan) for assistance in measurements. A. Adhikari and G. Zussman wish to acknowledge the support through NSF grants EEC- 2133516, CNS-2148128, AST-2232455. M. A. Almendra, M. Rodriguez, and R. Feick wish to acknowledge the support received from the Chilean Research Agency ANID, through research grants ANID FONDECYT 1211368, and ANID PIA/APOYO AFB230003; and the project VRIEA-PUCV 039.367/2023.

REFERENCES

[1] R. Cager, D. LaFlame and L. Parode, "Orbiter ku-band integrated radar and communications subsystem", IEEE Transactions on Communications, vol. 26, no. 11, pp. 1604-1619, Nov. 1978.

[2] C. W. Rossler, E. Ertin and R. L. Moses, "A software defined radar system for joint communication and sensing," 2011 IEEE RadarCon (RADAR), Kansas City, MO, USA, 2011, pp. 1050-1055.

[3] M. Alloulah and H. Huang, "Future Millimeter-Wave Indoor Systems: A Blueprint for Joint Communication and Sensing," in Computer, vol. 52, no. 7, pp. 16-24, July 2019.

[4] T. Wild, V. Braun and H. Viswanathan, "Joint Design of Communication and Sensing for Beyond 5G and 6G Systems," in IEEE Access, vol. 9, pp. 30845-30857, 2021.

[5] "Feasibility Study on Integrated Sensing and Communication (Release 19)", 3GPP TR 22.837 V19.1.0 (2023-09), Technical Report, 3rd Generation Partnership Project; Technical Specification Group TSG SA.

[6] *Technical Specification Group Radio Access Network; Study on Channel Model for Frequencies From 0.5 to 100 GHz* (Release 17), 3GPP TR 38.901 v.17.0.0, March 2022.

[7] E. M. Vitucci, V. Degli-Esposti, F. Fuschini, J. S. Lu, M. Barbiroli, J. N. Wu, M. Zoli, J. J. Zhu, H. L. Bertoni, "Ray Tracing RF Field Prediction: An Unforgiving Validation", International Journal of Antennas and Propagation, vol. 2015.

[8] R. Yang, C. -X. Wang, J. Huang, E. -H. M. Aggoune and Y. Hao, "A Novel 6G ISAC Channel Model Combining Forward and Backward Scattering," in IEEE Transactions on Wireless Communications, doi: 10.1109/TWC.2023.

[9] Z. Zhang et al., "A General Channel Model for Integrated Sensing and Communication Scenarios," in IEEE Communications Magazine, vol. 61, no. 5, pp. 68-74, May 2023

[10] A. Bhardwaj, D. Caudill, C. Gentile, J. Chuang, J. Senic and D. G. Michelson, "Geometrical-Empirical Channel Propagation Model for Human Presence at 60 GHz," in IEEE Access, vol. 9, pp. 38467-38478, 2021.

[11] D. Chizhik, J. Du, M. Kohli, A. Adhikari, R. Feick; R. A. Valenzuela, "Accurate Urban Path Loss Models Including Diffuse Scatter", 17th European Conf. on Antennas and Prop. (EuCAP), Florence, Italy, 2023.

[12] G. T. Ruck, D. E. Barrick, W. D. Stuart, C. K. Krichbaum, *Radar Cross Section Handbook*. Volumes 1 & 2, Plenum Press, January 1, 1970.

[13] D. Chizhik, J. Du, R. Feick, M. Rodriguez, G. Castro, and R. A. Valenzuela, "Path loss and directional gain measurements at 28 GHz for non-line-of-sight coverage of indoors with corridors", *IEEE Trans. Antennas Propag.*, vol. 68, no. 6, pp. 4820–4830, Jun. 2020.

[14] *IEEE 802.11 Wireless LANs Channel Models for WLAN Sensing Systems*, IEEE 802.11-21/0782r5, August 2021.

[15] N. Varshney, J. Wang, C. Lai, C. Gentile, R. Charbonnier and Y. Corre, "Quasi-Deterministic Channel Propagation Model for an Urban Environment at 28 GHz," in IEEE Antennas and Wireless Propagation Letters, vol. 20, no. 7, pp. 1145-1149, July 2021.

[16] D. Gubelli, O. A. Krasnov and O. Yarovyi, "Ray-tracing simulator for radar signals propagation in radar networks," *2013 European Radar Conference*, Nuremberg, Germany, 2013, pp. 73-76.

[17] D. Chizhik et al., "Average Backscatter Clutter Power for RF Sensing Applications in Indoor Environments," *2024 IEEE International Conference on Microwaves, Communications, Antennas, Biomedical Engineering and Electronic Systems (COMCAS)*, 2024.